

# Investigations Towards Ultra-Low Cost Nb<sub>3</sub>Sn SRF Cavity Fabrication via Melt Casted Bronze Route Processing

C. M. Rey<sup>1</sup>, G. Eremeev<sup>2</sup>, and Anne-Marie Valente-Feliciano<sup>3</sup>

**Abstract**—A novel approach to fabricating Nb<sub>3</sub>Sn SRF cavities and other RF components using an ultra-low-cost melt casting fabrication process has been investigated. This simple, low cost melt casting technique has the potential to be used to fabricate nearly any superconducting Nb<sub>3</sub>Sn structure using either the Bronze Route (BR), Internal Tin (IT), External Tin (ET) processes as well as normal conducting pure copper (Cu) cavities.

Most of the heat treated samples that were examined using SEM/EDX seemed to show a reasonable correlation of T<sub>c</sub> onset and transition width ( $\Delta T_c$ ) of the ingots initial/starting Sn content to the desired stoichiometric Nb<sub>3</sub>Sn phase, where the lower starting Sn content coupons resulted in lower T<sub>c</sub>'s with broader transition widths and the higher starting Sn coupons resulted in higher T<sub>c</sub>'s with narrower  $\Delta T_c$ 's. The best samples had T<sub>c</sub> onsets  $\sim$ 17–18 K and  $\Delta T_c$ 's  $< 2$  K. Two samples were further tested for RF surface resistance (R<sub>s</sub>) and Quality Factor (Q) at JLAB. These RF measurements were performed at 7.4 GHz using a calorimetric technique and showed two transitions, one at  $\sim$ 8 K and another at  $\sim$ 14 K; values of R<sub>s</sub> were at least two orders of magnitude higher than similar high quality Nb<sub>3</sub>Sn films directly deposited substrates by JLAB and with another superconducting transition close to the superconducting transition temperature of niobium. Substantial improvements in the processing variables ranging from higher quality of the initial ingots with higher Sn content, to better electro-polishing and reaction heat treatment regimens will be necessary to realize improved RF performance metrics.

**Index Terms**—Bronze Route, Nb<sub>3</sub>Sn, SRF Cavity

## I. INTRODUCTION

Energy to Power Solutions (e2P) in collaboration with the Thomas Jefferson National Accelerator Facility (JLAB), ExOne Corporation,[1] and the Hackett-Brass Foundry,[2] investigated a novel approach to Nb<sub>3</sub>Sn SRF cavity fabrication using synergistic technologies consisting of high quality Nb thin films deposited using (JLAB's) Electron Cyclotron Resonance (ECR) RF sputtering on low cost bulk “melt-casted” bronze (Cu-Sn) substrates/coupons. The starting bronze substrates were obtained using a two-step fabrication process consisting of first 3D printing a “sand mold” and then subsequent-

ly melt casting the bronze substrate using the 3D printed sand mold. A single-step process involving direct metal 3D printing with subsequent molten “bronze infusion” although possible, was not selected due to its far higher cost and significantly longer fabrication time.

e2P's patent pending Nb<sub>3</sub>Sn SRF cavity fabrication process (see US 62/087557 and 62/631,067) can be thought of as the “inverse” process of existing state-of-the-art technology[3] (i.e. Sn diffused into a bulk Nb cavity). In our modified Bronze Route (BR) process, the Sn content is provided by a near “infinite” reservoir from the underlying low cost ( $<\$3/\text{lb}$ ) bulk bronze (Cu-Sn) scaffold via high temperature reaction diffusion and the higher cost Nb is provided via (thin  $\sim 1\mu\text{m}$ ) film ECR deposition. In this study, multiple samples from five starting Cu:Sn alloys (89%Cu:11%Sn, 87%Cu:13%Sn, 86%Cu:14%Sn, 85%Cu:15%Sn, and 81%Cu:19%Sn) were subjected to our modified BR Nb<sub>3</sub>Sn fabrication process, which is summarized in section II-A. The technical feasibility of each step of our BR process was investigated on coupon sized samples. Thus far, the technical viability of the melt casting process appears to be encouraging and worthy of further study since our two-step melt casting technique can be similarly extended to pure Cu RF structures as well. If pure Cu cavities can be fabricated using our two-step process (i.e. 3D printed “sand” mold + Cu melt casting), this opens up the possibility of Nb<sub>3</sub>Sn SRF cavity fabrication via the more complex Internal Tin (IT) and External Tin (ET) processes as well as normal conducting Cu cavities and other related RF components. The melt casting process itself is well understood and dates back millennia. If technical viability can be shown, this technique could be used to fabricate large, complex structures (e.g. 9-cell RF cavity), at very low costs; however significant technical challenges remain for RF applications.

## II. EXPERIMENTAL

### A. Processing Parameters

At a high level, the seven step process used to fabricate the samples/coupons in our investigation is summarized below.

- Step 1: 3D Printing of Sand Molds for Bronze Substrates
- Step 2: Melt Cast Bronze Substrates in Sand Molds
- Step 3: Mechanical/Electro-Polishing Casted Substrates
- Step 4: Deposit Nb Thin Films on Bronze Casted Substrates
- Step 5: In Situ or Ex-Situ Post Reaction Heat Treatment
- Step 6: Test & Evaluate

This work was supported by the US DOE under contract DE-SC00018713. (Corresponding author: C.M. Rey.)

C. M. Rey is with Energy to Power Solutions (e2P), Tallahassee, FL 32304, USA (e-mail: cmrey@e2pco.com).

G. Eremeev was with Thomas Jefferson National Accelerator Facility, Newport News, VA 23606, USA. He is now with Fermi National Accelerator Laboratory, Batavia, IL, 60510, USA (e-mail: grigory@fnal.gov).

Anne-Marie Valente-Feliciano is with Thomas Jefferson National Accelerator Facility, Newport News, VA 23606 USA (e-mail: valente@jlab.org).

Color versions of one or more of the figures in this paper are available online at <http://ieeexplore.ieee.org>.

Digital Object Identifier will be inserted here upon acceptance.

### Step 7: Repeat process for DC/RF materials optimization

Our novel Steps 1 and 2 were quite straight forward, and from start to finish these two steps took < 1 week to fabricate all samples used in the investigation, with the majority of the time lost in shipping the samples from one place to the next. Optimizing the multitude of parameters and processing variables involved in Steps 3, 4 and 5 to obtain the correct  $\text{Nb}_3\text{Sn}$  stoichiometric ratio with good DC/RF properties were the key technical challenges in our initial 6 month investigation and where future R&D efforts should concentrate. Unfortunately, although there is extensive information available in the technical literature for each of these three steps (e.g. electro-polishing, Nb film deposition, and heat treatment) direct application to our modified BR process for SRF applications was not straightforward. For example, in Step 3, the vast majority of the literature for electro-polishing on pure Cu substrates proved of limited value as the established procedures developed for pure Cu cavities were for the most part inadequate for the bronze substrates. Furthermore, the diffusion reaction heat treat regimens developed over decades[4] for BR wire processing[5][6][7][8] were mostly geared towards small grains (hence high  $J_c$ ) operating in the vortex state[9] and not the desired larger grains used in SRF applications.[10]

In summary, e2P processed twenty 10x10 mm square samples for  $T_c$  measurements and thirteen 2" round samples for RF measurements. All of the 10x10 mm square substrates (cut from the original 2" diameter samples) and four of the thirteen 2" round substrates had their Nb films deposited with ECR at JLAB using high bias voltages (i.e. incident ion energies) of -60 V and -120 V. The remaining nine 2" diameter round samples had their Nb films (~1 $\mu\text{m}$ ) deposited with the more common low ion energy (< 10 eV) RF sputtering. In this paper, we only report measurement data and analysis on the bronze substrates with Nb films deposited with ECR at JLAB. The remaining nine samples with low ion incident energy RF sputtering were not heat treated due to time and fiscal limitations.

Processing variables investigated included: a) bronze type (Cu:Sn ratio), b) heat treatment temperature (700-800°C),[11] c) heat treatment environment vacuum vs. inert Argon, and d) Nb film deposition bias voltage (i.e. ECR ion incident energy). To avoid any ambiguity, a pure Nb film was deposited on each bronze substrate via the high ion energy ECR process, and not a  $\text{Nb}_3\text{Sn}$  film. The Nb coated bronze substrates were then heat treated/reacted in a separate reaction furnace (i.e. "Ex-Situ") to allow the Sn from the bronze to diffuse into the Nb via the BR solid state reaction process. Unfortunately, "In-Situ" BR processing with elevated bronze substrate temperatures (i.e. 100°C → 900°C) was not possible during this initial investigation for a variety of reasons including the concern over possible contamination of JLAB's ECR chamber. Subsequent R&D investigations should definitely explore this processing variable to determine its potential impact on  $\text{Nb}_3\text{Sn}$  stoichiometry, grain structure, and ultimately DC/RF properties.

### B. Sample Preparation

To better understand our  $\text{Nb}_3\text{Sn}$  BR fabrication approach, a typical sample preparation process is described. In the first step of the process, a 3D CAD drawing of the desired object is made. Once converted to the appropriate file type, the CAD drawing is sent to the 3D printer which then prints a "sand mold" for the object. In our investigation, two types of sand molds were fabricated: a) 2" diameter round substrates/cookies and b) dog-bone shaped samples for ASTM E8 tensile testing (see Fig. 1).



Fig 1: Bottom half of 3D printed sand molds

The sand molds were then used to melt cast the bronze coupons and subsequently discarded after one use. Of the five starting bronze ingots, only the 89/11 was commercially available. The remaining four bronze ingots with the higher starting Sn content had to be specially fabricated for this study. This turned out to be a serious detriment, since the quality of these R&D grade samples was quite poor possessing numerous pores, pits, and unevenly mixed Sn throughout its entire cross section (see Fig. 2).



Fig. 2: Comparison of an R&D grade bronze ingot to a commercial grade ingot. Note, the numerous pits and inadequate mixing of the starting Sn.

After the coupons had been melt casted into the 2" diameter substrates, their surface was quite rough and had to be mechanically polished by hand at e2P. While the lower Sn content commercial grade 89/11 substrates were relatively straightforward to polish, the higher Sn content R&D grade proved quite difficult as the pits/pores and poor Sn mixing seemed to permeate throughout the sample regardless of the amount of material removed from the surface. This turned out to be quite unfortunate as the samples that proved easiest to mechanically polish also turned out to have a too low starting Sn content that resulted in the lowest  $T_c$ 's. After mechanical polishing at e2P, the substrates were then sent to JLAB for electro-polishing. After electro-polishing the samples were ultrasonically cleaned, rinsed with ultra-pure water, dried in ISO6 cleanroom, and placed in the ECR chamber at JLAB. During the ECR deposition, the bronze substrates were not independently heated, with the only heating stemming from the incident ions of the ECR sputtering process. In-Situ substrate heating is a processing variable that needs further investigation. During Nb film deposition, two different bias voltages

were studied: -60 V and -120 V. Our target Nb film thickness was  $\sim 1 \mu\text{m}$ . After Nb film deposition, some of the samples were sent back to e2P and some remained at JLAB. A selected few of the JLAB Nb coated samples were analyzed using SEM/EDX. Others were loaded into their vacuum furnace for post reaction heat treatment. The Nb coated samples that were sent to e2P underwent a  $T_c$  measurement and then were loaded into a post reaction heat treatment in an inert Ar atmosphere. After heat treatment, samples once again underwent  $T_c$  testing. Two of the vacuum heat-treated samples underwent RF testing at JLAB.

The post reaction heat treatment regimens are another R&D area that needs significant optimization. As mentioned, the technical literature provided little guidance for an optimized post reaction heat treatment regimen that optimized Meissner state RF properties. Furthermore, the short duration of the investigation did not allow for long protracted heat treatments. In this study, time durations were in general limited to  $< 48$  hours from start to finish and reaction temperature to a single uniform temperature in the range of 700-800°C (see Table I). Temperatures higher than 800°C were attempted on one run; however, since multiple samples of varying Sn content substrates were being reacted in a single chamber, partial melting of the 81%Cu/19%Sn sample resulting in contamination of all the samples which had to be discarded.

### C. Measurement and Analysis

Time and fiscal restraints of the effort limited the types of testing and analysis that could be performed. All post reacted samples of reasonable visual quality (i.e. no flaking/peeling) were initially tested for its  $T_c$  using an AC inductance technique. Up to five (5) samples could be loaded onto a specially designed sample holder which was attached to the 2<sup>nd</sup> stage of GM cryocooler. To initially calibrate the  $T_c$  measurement apparatus, AC inductance measurements were taken as a function of temperature using pure Pb, pure Nb, and 2G YBCO thin films all of similar thicknesses ( $\sim 1-3 \mu\text{m}$ ). The samples  $T_c$ , defined here as its onset temperature, its transition width ( $\Delta T_c$ ), and diamagnetic response via its change in inductance value ( $\Delta L = L_f - L_i$ ) were used to characterize the three calibration samples. To characterize the temperature lag between the Cernox® sensor and sample itself, measurements were taken both on cooldown (i.e. decreasing T) and warm-up (i.e. increasing T) and subsequently averaged. The pure Pb and Nb thin films showed a  $T_c$  onset within  $\sim 0.2$  K of the literature value and the 2G YBCO film had an onset  $T_c \sim 91$  K. All three calibration samples had a transition width  $\Delta T_c < 1$  K, and an inductance change  $\Delta L \sim 25 \mu\text{H}$ . The manufacturer stated accuracy of the Cernox® sensor was  $\sim 0.5$  K.

## III. TEST RESULTS

### A. AC Inductance Measurements

Once the AC inductance measurement technique was verified and calibrated, tests were then performed on the smaller

10x10 mm heat treated Nb<sub>3</sub>Sn samples. Fig 3 shows a typical diamagnetic response from a 86%Cu: 14%Sn 10x10mm sample. The two red, dashed lines demarcate the temperature transition width ( $\Delta T_c$ ). Both the initial cooldown (decreasing T) and warm-up (increasing T) measurements were used to determine if there was a “lag” between sample temperature measurement and actual sample temperature. The difference in  $T_c$  onset between initial cool-down and warm-up measurements was typically  $< 0.5$  K.

In addition to the ‘primary transition,’ the majority of the results (not all) showed a substantial ‘tail’ in the transition

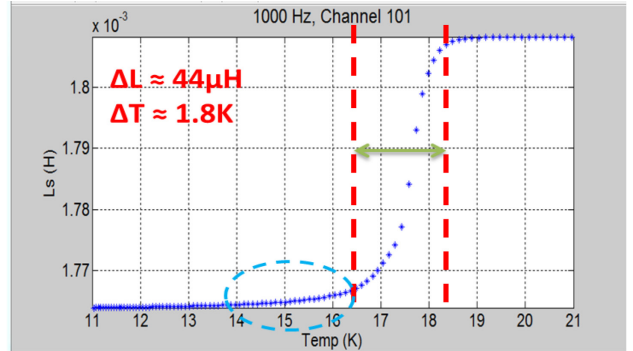


Fig. 3. Diamagnetic response of a 86%Cu/14%Sn 10x10 mm sample with  $T_c \sim 18$  K,  $\Delta T_c \sim 1.8$  K, and  $\Delta L \sim 44 \mu\text{H}$ .

width (see blue dashed circle). While we believe that this could be an indication of some non-stoichiometric low Sn content from the reaction diffusion process, this long tail was also observed in all of the pure ECR deposited Nb films prior to heat treatment, albeit at lower temperatures ( $\sim 4 \rightarrow 6$  K). Some samples showed a smaller secondary transition at  $T_c \sim 9$  K (not observed for sample shown in Fig. 3) indicating that a portion of the pure Nb film was not converted to the Nb<sub>3</sub>Sn phase. The Nb film thickness is obviously another variable that requires further optimization in this modified BR process.

Interestingly, the magnitude of the diamagnetic response for many of the higher quality (i.e. higher final at wt. Sn content per EDX analysis) heat treated Nb<sub>3</sub>Sn films showed a  $\Delta L \sim 30-45 \mu\text{H}$ , when compared to the  $\Delta L \sim 25 \mu\text{H}$  for the three calibration thin films. While there are several possible reasons for this larger diamagnetic response in the heat treated Nb<sub>3</sub>Sn samples, one possible explanation could be that the reaction diffusion process may be converting a larger volume fraction of material to the superconducting Nb<sub>3</sub>Sn phase than just at the initial surface of the  $\sim 1 \mu\text{m}$  Nb film surface. A summary of the AC susceptibility test results for the 10mm x 10mm samples is shown in Table I. In general, test results were quite encouraging yielding  $T_c$  onset values ranging from  $\sim 15$  K  $\rightarrow 18.3$  K with reasonably sharp transition widths  $\Delta T < 2$  K for many of the samples. For the highest quality Nb<sub>3</sub>Sn samples, (i.e. those with the highest net post reacted at. wt. % Sn content), transition widths were extremely sharp with  $\Delta T < 1$  K. We are particularly encouraged by these promising results especially in light of the very short time duration of the study and the entirely new fabrication melt casted process.

TABLE I: Summary of Properties on 10x10 mm samples

| Bronze               | Sample Name | Nucleation Voltage (V) / Ion Energy (eV) | Heat Treatment | Soak Temperature (C) | T <sub>c</sub> / Transition Width ΔT (K) | Inductive Signal Strength ΔL (μH) |
|----------------------|-------------|--|----------------|----------------------|--|-----------------------------------|
| C907<br>Cu/Sn: 89/11 | 907-1       | -120/184                                 | HT1            | 700                  | NA                                       | NA                                |
|                      | 907-2       | -60/124                                  | HT4            | 759                  | 15.2/1.3                                 | 23 ± 7                            |
|                      | 907-3       | 0/64                                     | HT6            | 798                  | 14.8/1                                   | 8                                 |
|                      | 907-4       | -240/304                                 |                |                      |  |                                   |
| C909<br>Cu/Sn: 87/13 | 909-1       | -120/184                                 | HT1            | 700                  | NA                                       | NA                                |
|                      | 909-2       | -60/124                                  | HT4            | 759                  | 17.3/1                                   | 30 ± 7                            |
|                      | 909-3       | 0/64                                     | HT6            | 798*                 | 17.6/1.3                                 | 33 ± 10                           |
|                      | 909-4       | -240/304                                 |                |                      |  |                                   |
| C910<br>Cu/Sn: 85/15 | 910-1       | -120/184                                 | HT1            | 700                  | 18.3/0.8                                 | 0.35 ± 0.2                        |
|                      | 910-2       | -60/124                                  | HT4            | 759                  | 18.1/1.3                                 | 29 ± 7                            |
|                      | 910-3       | 0/64                                     | HT6            | 798*                 | 16.9/1.6                                 | 21 ± 10                           |
|                      | 910-4       | -240/304                                 |                |                      |  |                                   |
| C911<br>Cu/Sn: 84/16 | 911-1       | -120/184                                 | HT2            | 700                  | 17.5/1.4                                 | 35 ± 8                            |
|                      | 911-2       | -60/124                                  | HT5            | 700                  | 16.2/1.2                                 | 32 ± 3                            |
|                      | 911-3       | 0/64                                     | HT7            | 759                  | 15.8/0.9                                 | 17 ± 10                           |
|                      | 911-4       | -240/304                                 |                |                      |  |                                   |
| C913<br>Cu/Sn: 81/19 | 913-1       | -120/184                                 | HT3            | 700                  | 16.6/0.9                                 | 28 ± 15                           |
|                      | 913-2       | -60/124                                  | HT7            | 759                  | 15.5/1.7                                 | 31 ± 4                            |
|                      | 913-3       | 0/64                                     | HT7            | 759                  | 16.0/1.4                                 | 26 ± 4                            |
|                      | 913-4       | -240/304                                 |                |                      |  |                                   |

\*Soak temperature seemed to be too hot for these samples: they appeared slightly melted after heat treatment

### B. SEM/EDX Analysis

A select few of the pre and post heat treated samples underwent SEM/EDX analysis at JLAB (see Fig. 4). Shown in Fig. 4 is a series of SEM photographs on a 2" diameter 907 (i.e. 89% Cu/11% Sn) coupon heat treated for 24hr at 700°C in vacuum. EDX analysis of the surface reveals two interesting features. First, the small (~5μm) grains on the surface of the sample are Cu rich precipitates. Second, the smooth regions containing no Cu-rich precipitates show an under stoichio-

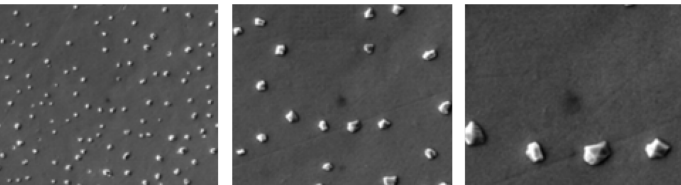


Fig. 4: SEM photographs at 50, 20, and 10μm on a 2" diameter 907 (89/11 Cu/Sn) coupon post 700°C vacuum furnace heat treatment

metric Sn content of ~15% relative to the desired 25% for optimal RF properties. The lower values of T<sub>c</sub> are most likely due to lower than ideal post reacted at wt. % Sn content for under stoichiometric Nb<sub>3</sub>Sn.[12] Although more SEM/EDX data is needed to confirm this hypothesis, the select few samples in which SEM/EDX measurements were taken show post reacted Sn contents varying between 8% and 24% (with ideal =25%), with the majority of the lower T<sub>c</sub> samples resulting from the commercial grade 89% Cu/11% Sn ingot, which had the lowest starting Sn content of the bronze substrates. We caution the reader of the potential for confusion regarding the initial starting Sn % content of the starting bronze ingot compared to the final post reacted at. % Sn of the Nb<sub>3</sub>Sn as measured by EDX.

### C. RF Measurements

Two vacuum heat-treated 89%Cu/11%Sn samples were further tested for RF surface resistance (R<sub>s</sub>) and Q at JLAB. These RF measurements required a 2" diameter substrate (i.e. not the 10x10 mm) and were performed at 7.4 GHz using a calorimetric

technique developed at JLAB.[13] These RF measurements showed two transitions at about 8 K and 14 K, with values of R<sub>s</sub> about at least two orders of magnitude higher than similar high quality Nb<sub>3</sub>Sn films directly deposited substrates by JLAB. This corresponds reasonably well with the poor performance observed in the AC inductance measurements of T<sub>c</sub>. As a reminder, the commercial grade 89%Cu:11%Sn samples were initially selected for RF evaluation based upon their relative ease to mechanically polish and not its T<sub>c</sub> value. It is unfortunate that time and funds of the investigation were exhausted before 2" diameter samples (required for RF measurements) with starting Sn contents > 87%Cu/13%Sn were fabricated, since their T<sub>c</sub>, ΔT<sub>c</sub>, and ΔL properties on the 10x10 mm squares were superior (see Table I). It would be interesting to see the relative effect on R<sub>s</sub> and Q values, when comparing lower starting Sn content with superior surface finish to higher starting Sn content with inferior surface finish.

### IV. SUMMARY

While this initial investigation did demonstrate technical viability of the melt casting approach to some degree, there are several areas that need to be addressed in future R&D investigation in order to realize substantial improvements in RF performance. The first two steps in our BR fabrication process that did go quite smoothly. The 3D printed sand molds used in the melt casting proved to be relatively straight forward. This step was simple, quick, and low cost. In future R&D investigations, direct 3D printing of the metal matrix with subsequent “bronze infusion” will also be investigated. The bronze melt casting also proved to be relatively straight forward once the starting ingots were obtained. Future R&D investigation will require higher quality, void free, homogenous ingots with Cu/Sn ratios > 87/13. In addition, better electro-polishing methods and optimized heat treatment regimens are needed for correct stoichiometric Nb<sub>3</sub>Sn phase formation.

### REFERENCES

- [1] See [www.ExOne.com](http://www.ExOne.com).
- [2] See [www.hacketbrass.com](http://www.hacketbrass.com).
- [3] G Müller et al. “Nb<sub>3</sub>Sn Layers on High Purity Nb Cavities with Very High Q Factors,” Proc. EPAC96, Barcelona, Spain, pp. 2085-2087, 1996.
- [4] K. Tachikawa and P.J. Lee, History of Nb<sub>3</sub>Sn and Related A15 Wires,” Taylor & Francis, (2011).
- [5] M. Suenaga et al. “The Fabrication and Properties of Nb<sub>3</sub>Sn Bronze Route Solid Diffusion Process,” *IEEE Trans. Mag.*, vol. MAG-11, 2, March 1975.
- [6] I.M. Abdyukhanov et. al, *IEEE Trans. Appl. Supercon.*, Vol 22, No. 3, 2012.
- [7] Popova E.N., Deryagina I.L., Valova-Zaharevskaya E.G. *Cryogenics*, Vol. 63, p. 63-68, 2014.
- [8] I. Deryagina, E. Popova, E. Patrakov, et al. *IEEE Trans. Appl. Supercond.*, Vol. 28, No. 4, 2018.
- [9] L. D. Cooley, P.J. Lee, and D.C. Larbalestier, *Proceed. Int. Cryogenic Mat. Conf.*, vol. 48, pp.925-932, 2002.
- [10] A. Godeke et al., “Nb<sub>3</sub>Sn for Radio Frequency Cavities,” <https://escholarship.org/uc/item/6d3753q7>, Dec. 2006.
- [11] E. Valova-Zaharevskaya, E. Popova, I. Deryagina, et al. *IEEE Trans. Appl. Supercond.*, Vol. 28, No. 4, 2018.
- [12] E. Barzi and A. Zlobin, Fermilab pub. 15-274-TD-007, (2015).
- [13] B.P. Xiao et al., “Calorimetric Measurements on SRF Samples,” *Rev. Sci. Instru.*, 83, 124905, 2012.